Finite Element Analysis of Planar Inductors with Soft Magnetic Encapsulation Materials

Wang, Jiaxuan; Li, Xiao; Zhao, Jiayan; Li, Jinbing; Zhang, Guoqi; Liu, Pan

DOI
10.1109/ICEPT63120.2024.10668611

Publication date
2024

Document Version
Final published version

Published in
2024 25th International Conference on Electronic Packaging Technology, ICEPT 2024

Finite Element Analysis of Planar Inductors with Soft Magnetic Encapsulation Materials

1st Jiaxuan Wang
Academy for Engineering and Technology
Fudan University
Shanghai, China
jiaxuanwang22@m.fudan.edu.cn

2nd Xiao Li
Academy for Engineering and Technology
Fudan University
Shanghai, China
xiao_li21@m.fudan.edu.cn

3rd Jiayan Zhao
Department of Research and Development
Mazo Technology Company Limited
Kunshan, China
kevin_chao@mazotech.com

4th Jinbing Li
Department of Research and Development
Mazo Technology Company Limited
Kunshan, China
dylan_li@mazotech.com

5th Guoqi Zhang
Electronic Components, Technology, and Materials
Delft University of Technology
Delft, the Netherlands
g.q.zhang@tudelft.nl

6th Pan Liu*
Academy for Engineering and Technology
Fudan University
Shanghai, China
Research Institute of Fudan University in Ningbo
Ningbo, China
panliu@fudan.edu.cn

2024 25th International Conference on Electronic Packaging Technology (ICEPT) | 979-8-3503-5380-8/24/$31.00 ©2024 IEEE | DOI: 10.1109/ICEPT63120.2024.10668611

***Abstract*—The rise of 5G, artificial intelligence, and other applications drives the demand for planar inductors based on PCB processes, due to the advantages of compatible processes, flat shapes, high power densities, reduced volumes, etc. In this paper, six kinds of soft magnetic encapsulation materials (SMEs) were selected to prepare planar dual-layer spiral inductors (PDSI). The actual PDSI device, as well as the six kinds of SMEs, were then processed. Based on the tested relative permeability of SMEs, FEM models were built and calibrated through the actual PDSI structures. Furthermore, FEM models of single-layer, double-layer, and multilayer inductors were established respectively, with analysis of the differences in magnetic properties. The results reveal that both L and Q of the PDSI exhibit a positive linear correlation with the relative permeability of the SMEs, and SMEs with high permeability limit the magnetic leakage. The multilayer inductor could achieve similar *L* and *Q* values with a smaller area compared with the planar inductor. However, the increase in thickness limits their application in thin devices. The models can be adjusted to match the SME properties and size parameters of the actual manufacturing process, contributing to simplified calculations for inductor design and performance analysis. Based on such analysis, the planar inductor designs based on in-house SME and PCB-compatible processes are adjusted for high-frequency applications.**

Keywords—Finite element method, Planar spiral inductor, Multilayer inductor, Soft magnetic encapsulation materials

I. Introduction

The demand for miniaturization, high efficiency, and high power density in power electronics has been increasing with the rise of 5G, electric vehicles, and aerospace applications [1]. With the size shrinkage of active power chips, the passive components face continuous challenges for size reduction, especially for inductors [2]. Compared with the continuous size reduction of active devices, inductors tend to occupy more volume in the system, due to the limitations of their structures [3]. To overcome the traditional bulky ones, inductors are under development towards planarization, system integration, and high-frequency work ranges [4, 5]. Among the under-developed inductors, molded inductors are popular for high working frequency applications, with compact structures made by winding wire on coil skeletons or magnetic cores. It is usually followed by cold pressing or hot pressing with magnetic powder. However, due to the limitations of the winding preparation process, when it is prepared on a size of less than 1 mm^2, the problem of skeleton or coil fracture often occurs during the molding process, thus limiting its application in high-frequency devices [6].

Unlike traditional molded inductors, planar inductors based on the PCB processes are attractive with compatible processes, flat shapes, high power densities, reduced volumes, lightweight, and better heat dissipation performance [7]. The magnetic material that encapsulates the inductor coil with high permeability enhances the conduction ability of the magnetic field to improve the inductance value. It also helps to optimize the coil structure, such as the downsizing of the inductor by reducing the number of turns of the coil and the volume of the magnetic material. However, challenges still remain. On one hand, the permeability of soft magnetic encapsulation materials (SMEs) compatible with the PCB process is lower than the inductance of traditional molded inductor cores [8]. On the other hand, SMEs are usually under high tackiness which brings difficulties for processing.

Therefore, a planar dual-layer spiral inductor (PDSI) based on PCB technology was proposed in this paper. The influence of different magnetic packaging materials was analyzed by finite element method (FEM). The effects of different structures of conventional single-layer inductors, dual-layer inductors, and multilayer inductors on inductor performance were compared and analyzed, which demonstrated the advantage of SME-embedded multi-layer inductors based on PCB processes.

II. Inductor Preparation

In this work, the desired inductor based on PCB processes includes SEM and copper coils. For FEM analysis of such devices, the relative permeability of SME, as well as the PDSI structures, need to be characterized and optimized.

TABLE I. SELECTED MAGNETIC POWDERS

Category	D-50	Brand
Carbonyl iron powder	6 μm	RZEL
FeSiCr alloy	10 μm	ATA
Fe-based amorphous alloy	21 μm	AMP-2
Fe-based amorphous alloy	10 μm	WNPM02
Fe-based amorphous alloy	38 μm	ONAM
Fe-based Nanocrystalline alloy	14 μm	NC1

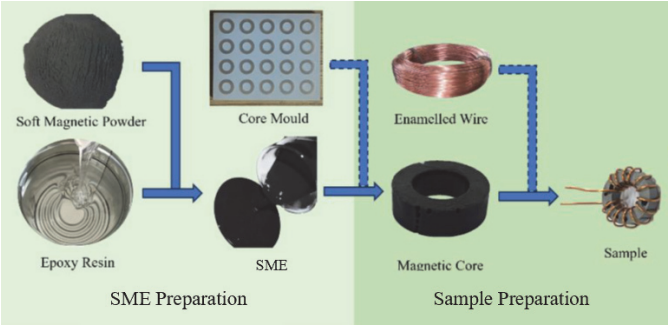

Fig. 1. The preparation process of the relative permeability test samples

A. The Relative Permeability Measurement of SME

The SMEs for the PDSI are mainly composed of soft magnetic powder and epoxy resin. The permeability of the magnetic materials is the focus of attention, since high permeability materials usually reduce the inductance winding, resulting in a lower DC resistance (DCR) to ensure the inductance value, thus further reducing the DC loss of the inductance [9]. In this paper, six kinds of magnetic powders were selected as presented in Table I. SMEs were obtained after mixing the powders with epoxy adhesive by vacuum stirring, respectively. The epoxy adhesive was prepared by E-51 epoxy resin, D-230 curing agent, and A-10 defoamer provided by Baling Petrochemical Company, with a mass fraction of 100:32:0.5. 85 wt% magnetic powders were added to ensure the fluidity met the processing requirements.

Toroidal magnetic cores with copper wire winding were prepared for the relative permeability measurement of the six SMEs. The preparation process is shown in Fig. 1. The SMEs, obtained by stirring the soft magnetic powder and epoxy adhesive, were placed into the Teflon core mold, and heated at 80 °C and 120 °C for 2 and 3 hours, respectively. After the preparation of the magnetic cores, the copper coils were wound, and their relative permeability was measured by LCR Meter, with the results presented in Fig. 2. NC1 SME possesses a significant advantage in permeability, reaching 14.6. The nanocrystalline magnetic powder has a fine grain size and a relatively uniform microstructure, which enables it to reduce the material's hysteresis loss and maintain a high relative permeability at high frequencies.

B. Preparation of the PDSI

The structure of PDSI designed in this work included five layers, as presented in Fig. 3, which are SME, coil, SME, coil, and SME (from top to bottom). The preparation scheme of PDSI in this work consists of three steps, which are:

- The preparation of double-sided copper-covered magnetic substrate;

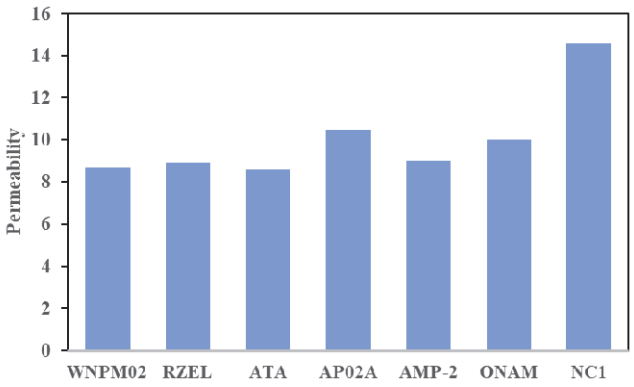

Fig. 2. The relative permeability of the SMEs

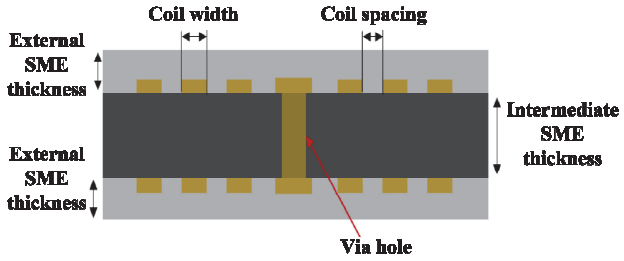

Fig. 3. Cross-section structure diagram of PDSI

- Etching of coil structure;
- Coating of external SMEs.

The process of the core step double-sided copper-coated substrate preparation is as follows:

- Put polypropylene cloth into a container with SME to infiltrate the PP cloth, then take it out.
- After wetting and drying, the intermediate magnetic layer is obtained.
- Place the copper foil and PP cloth impregnated with SME into the hot-pressing mold in the form of three layers of copper foil, PP cloth, and copper foil to make a magnetic double-covered copper substrate.

III. MAGNETIC ANALYSIS

A. Establishment of the Finite Element Model

In the magnetic simulation section, the inductance value, DC resistance, Q value, and magnetic flux density of the inductor will be focused. A PDSI model with a size of 6.60 mm × 6.60 mm × 1.55 mm and turns 2N=14 was built by SOLIDWORKS 2023 and then imported into COMSOL Multiphysics 6.2 for the finite element simulation. Detailed design parameters and model diagram are shown in Table II and Fig. 4 respectively.

The dual-layer planar spiral coils encapsulated by SME were placed in a sufficiently large air domain. The formulas required for inductance parameter calculation and model simulation are as follows.

The usual formula for calculating the inductance value is,

$$L = \mu_0 \mu_i N^2 A_e / l_e \quad (1)$$

where μ_0 is the vacuum permeability of $4\pi\times10^{-7}$H/m, μ_i is the relative permeability of the matrix material, and N is the

TABLE II. DESIGN PARAMETERS OF THE PDSI

Size (mm)		
Inductor	length	6.60
	width	6.60
	thickness	1.55
Coil	width	0.15
	spacing	0.20
	thickness	0.10
	layer spacing	0.55

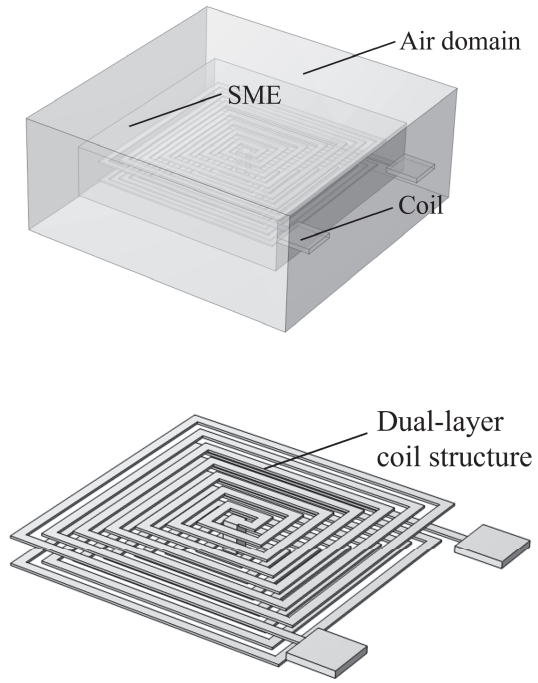

Fig. 4. The FEM model of the PDSI

number of turns of the coil. *Ae* is the effective cross-section enclosed by the inner electrode coil, and *le* is the effective length of the inner electrode coil.

The quality factor Q represents the ratio of energy storage to energy consumption of the laminated chip inductor substrate. Its calculation is expressed as

$$Q = 2\pi fL/R \tag{2}$$

where f is the test frequency, and L and R are the inductance value and the equivalent internal structure of the inductance at f frequency, respectively. The larger the Q value, the smaller the circuit loss, thus leading to the better the performance of the device.

The DCR of the inductor is also an important parameter of the inductance device, which is closely related to the inductance loss, and its calculation formula is

$$R_{DC} = \rho l/S \tag{3}$$

where ρ is the resistivity of the inductor conductor, l refers to the equivalent length of the inner electrode, and S refers to the equivalent cross-sectional area of the inner electrode.

TABLE III. MATERIAL MAGNETIC PARAMETERS

Material	Relative permeability	Relative dielectric constant	Electrical conductivity (S/m)
Copper coil	1	1	5.998e7
SME	x	3.5±	0
Air domain	1	1	0

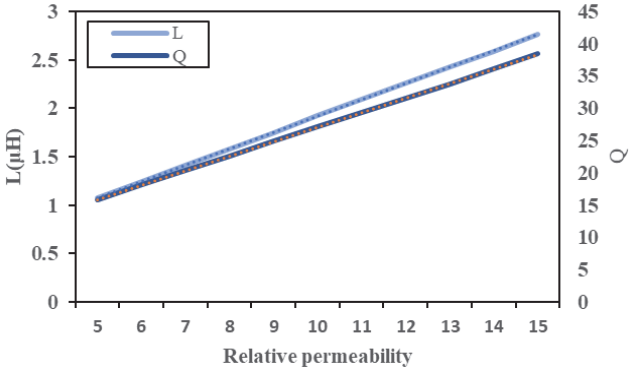

Fig. 5. Relationship curves of L, Q, and relative permeability.

Since the resistivity is fixed, the DCR is adjusted by the inner electrode thickness, width, and equivalent length, while it also causes changes in the inductance value.

B. FEM Simulation Results

The magnetic field interface of the AC/DC module in COMSOL was applied for the FEM simulation in this work. The input material performance parameters are shown in Table III. The relative permeability x was adjusted according to the materials, and the relative dielectric constant changed little. The simulation of L, Q, and magnetic flux density was carried out under 1 V voltage excitation and 1 MHz operating frequency.

In the FEM simulation, the variation range of relative permeability x was set from 5 to 15, including the above six kinds of SMEs. The simulation results of inductance value L and quality factor Q are shown in Fig. 5. Both L and Q are positively correlated with x. Therefore, their fitting curves equation in this model can be summarized as follows:

$$L = 0.1692\,x + 0.9031 \tag{4}$$

$$Q = 2.2545\,x + 13.573 \tag{5}$$

Under the condition that the insulation, magnetic loss, and processability of SMEs meet the requirements, the higher the relative permeability, the better the magnetic properties of PDSI.

In terms of magnetic flux density, it can be seen from the comparison results in Figure 5 that with the increase of relative permeability, the magnetic flux density of inductors increases, and the uniformity of magnetic flux density distribution is not affected. In addition, the higher relative permeability inhibits the magnetic leakage phenomenon of inductors, since the magnetic flux density on the outside of the inductor decreases significantly.

PDSI samples were prepared according to the FEM simulation model data, as exhibited in Fig.7. The inductance value and quality factor of the sample were tested and the results in Table IV were obtained. There is a large gap

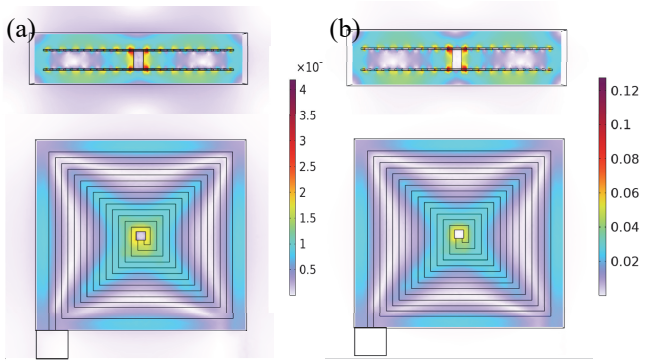

Fig. 6. Magnetic flux density simulation results of SMEs with a relative permeability of (a) 5 and (b) 15, respectively.

Fig. 7. Manufacture of PDSI.

TABLE IV. COMPARISON OF L AND Q BETWEEN SIMULATION AND TEST RESULTS

Method	L (μH)	Q
FEM simulation	1.56	19.5
Experiment test	1.24	17.2

between the simulation results and the test results of L and Q, reaching 20.5% and 11.8%, respectively.

There are three main reasons for this error: uneven epoxy distribution in the intermediate SME layer, inaccurate coil etching size, and non-dense SME coating structure. During the compaction of the double-sided copper-coated substrate, temperature, pressure, and flatness of the copper foil all affect the evenness and porosity of the substrate. Due to the small core size, the error of line width and spacing greatly influences the inductor performance. Since the external SMEs were prepared by a coating process, the introduction of bubbles due to PCB processes will cause a decrease in magnetic properties.

C. *Comparison among single, double, and multilayer inductors on magnetic performance*

Considering that the total inductance value of the multilayer inductor is composed of the self-inductance value of each coil layer and the mutual inductance between each layer, the total inductance value Lm can be expressed as follows if the winding direction of each layer is the same,

$$Lm = \sum_{i=1}^{n} Li + \sum_{i=1}^{n} \sum_{j=1}^{n} Lij \qquad (6)$$

where L_i is the self-inductance of each layer, and L_{ij} is the mutual inductance between each layer.

In this section, based on (1), (2) and (6), single-layer and multilayer inductors FEM models, in addition to the above PDSI model, were established to analyze the differences in magnetic properties between them, as presented in Fig. 8. In terms of the single-layer inductor, the geometry was kept unchanged, the number of layers was set to single layer, the coil thickness was increased by 2 times, and the other parameters remain unchanged. When the relative permeability was set to 10, the L of the single-layer inductor decreased to 0.83 μH, which was only 53.2% of the PDSI; however, Q resulted in 26.4 with an increase of 33.9%. The main reason is that the total inductance decreases due to the disappearance of interlayer mutual inductance, while the equivalent length of the coil decreases and the effective cross-sectional area increases, leading to a decrease in inductor resistance and then an increase in Q.

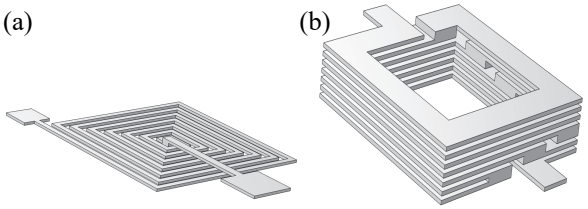

Fig. 8. The coli structures of (a) single-layer inductor and (b) multilayer inductor.

TABLE V. COMPARISON OF SIMULATION RESULTS OF THE THREE INDUCTORS

Inductor type	Size (mm)	L (μH)	L density (nH/mm³)	Q	DCR (mΩ)
Double-layer	6.6×6.6×1.55	1.56	23.1	19.5	199
Single-layer	6.6×6.6×1	0.83	19.1	26.1	52.9
Multi-layer	4.5×4.5×1.7	0.87	25.3	37.0	43.8

Compared with the coil structure of planar spiral inductors, the design of multilayer inductors with one turn per layer at most resulted in their thickness increase and inductance reduction. On the other hand, the design expanded the range of width adjustment of the coils, which could compensate for the disadvantage of L reduction by setting a wider coil. In the model established above with a size of 4.5 mm × 4.5 mm × 1.5 mm, the number of inductor layers was 7 (equivalent coil turns were 7), and the coil width and thickness were set to 0.5 mm and 0.05 mm, respectively. Table V presents the comparison of simulation results of the above three types of inductors. When the relative permeability of the magnetic material was 10, the inductance value of the multilayer inductor expressed 0.87 μH, which was consistent with that of the single-layer inductor. Q increased to 37.0 due to a further reduction in coil resistance. As a result, the multilayer inductor achieved similar L and Q values with about 50% of the single-layer inductor plane area, while the thickness increased 2-3 times. The lower resistance value was also conducive to the increase of current bearing and power of the inductor.

Due to the time limitation, this work only carried out the simulation results of the above three models. Further work is concentrated on the optimization of inductor parameters with performances. In addition, actual sample tests for single-layer and multi-layer capacitors will be planned in the future, as well as some key performance tests such as self-resonant frequency, saturation current, etc., to further demonstrate the possibilities of such PCB-based processes for high-frequency power inductor manufacturing.

IV. Conclusion

In this paper, planar dual-layer spiral inductors (PDSI) were prepared with six soft magnetic encapsulation materials (SMEs). Based on the actual PDSI devices, the influence of different SMEs on the magnetic properties, such as inductance *L*, quality factor *Q*, and magnetic flux density was analyzed by FEM. Models of single-layer, dual-layer, and multilayer inductors were established, and their magnetic properties were analyzed to identify the differences.

In the planar dual-layer spiral inductor model established in this work, both the *L* and *Q* presented a positive linear correlation with the relative permeability of the soft magnetic encapsulation materials. With the increase of relative permeability, *L*, *Q*, and magnetic flux density increase, and inductance magnetic leakage decreases. The *L* and *Q* of the PDSI were 1.56 μH and 19.5, respectively, with an SME applied at a relative permeability of 10. The simulation results for the L and Q of the single-layer inductor with the same specifications as the PDSI were 0.83 μH and 26.1, which indicated a decrease of 46.8% and an increase of 51.7%, respectively. The multilayer structure resulted in their thickness increase and inductance reduction, on the other hand, expanded the range of width adjustment of the coils, which could compensate for the disadvantage of L reduction by setting a wider coil. Compared to the single-layer inductor, the multilayer inductor model achieved similar values of L and Q with about 50% of the planar area.

Based on such simulation, the inductor specifications, such as coil size and SME properties, are adjusted according to the requirements of the PCB process. The future planned simulations and tests for self-resonant frequency, saturation current, and other parameters will further enhance this work.

Acknowledgment

The authors would like to thank the funding of the MAZO TECH-Fudan cooperation project, Shanghai SiC Power Device Engineering and Technology Research Center (19DZ2253400). Thanks also to ChatGPT for the assistance.

References

[1] P. A. Kyaw, A. L. F. Stein, and C. R. Sullivan, "Fundamental Examination of Multiple Potential Passive Component Technologies for Future Power Electronics," TPEL, vol. 33, no. 12, pp. 10708-10722, 2018.

[2] A. Zolfaghari, A. Chan, and B. Razavi, "Stacked inductors and transformers in CMOS technology," JSSC, vol. 36, no. 4, pp. 620-628, 2001.

[3] S. Gao and H. Wang, "A New Approach Integrated Magnetics Double-Frequency DC/DC Converter," Access, vol. 8, pp. 148301-148314, 2020.

[4] H. Ronkainen, H. Kattelus, E. Tarvainen, T. Riihisaari, M. Andersson, and P. Kuivalainen, "IC compatible planar inductors on silicon," IEE proceedings. Circuits, devices, and systems, vol. 144, no. 1, pp. 29-35, 1997.

[5] N. Zao et al., "Design and Analysis of Vertical Nanoparticles-Magnetic-Cored Inductors for RF ICs," TED, vol. 60, no. 4, pp. 1427-1435, 2013.

[6] J. He et al., "Soft magnetic materials for power inductors: State of art and future development," Materials Today Electronics, vol. 6, p. 100066, 2023.

[7] Y. Benhadda, M. Derkaoui, K. Mendaz, H. Kharbouch, and P. Spiteri, "Design for Integrated Planar Spiral Inductor for MEMS," Periodica polytechnica. Electrical engineering and computer science, vol. 67, no. 4, pp. 425-437, 2023.

[8] A. H. Shaltout and S. Gregori, "Layout optimization of planar inductors for high-efficiency integrated power converters," Analog Integr Circ Sig Process, vol. 102, no. 1, pp. 155-167, 2020.

[9] X. Li, J. Tang, J. Zhao, J. Li, G. Zhang, and P. Liu, "Finite Element Analysis of Power Module Packages with One-step Molding for Power Inductors," 2022: IEEE, pp. 1-5.